Solar Cells, *20* (1987) 51 - 57

A COMPARISON BETWEEN EXCIMER LASER AND THERMAL ANNEALING FOR ION-IMPLANTED POLYCRYSTALLINE SILICON SOLAR CELLS

W. SINKE, A. POLMAN and F. W. SARIS

FOM Institute for Atomic and Molecular Physics, Kruislann 407, 1098 SJ Amsterdam (The Netherlands)

(Received March 3, 1986; accepted August 28, 1986)

Summary

Polycrystalline silicon (Wacker–SILSO) solar cells have been made by phosphorus implantation in combination with pulsed excimer laser annealing or thermal annealing. It was found that laser annealing yields cells with a short-circuit current which is 3% - 4% higher than that obtained by thermal annealing, whereas the open-circuit voltage is the same for both cases. It was concluded from curve fitting that the current–voltage characteristics of all cells could be described well using a double-exponential model.

1. Introduction

Polycrystalline silicon (poly-Si) is considered to be an attractive alternative to single-crystal silicon as base material for the fabrication of solar cells. Using poly-Si, it is possible to achieve a noticeable reduction in cell price at the cost of a relatively small decrease in efficiency. For this reason, research is dedicated to the development of various kinds of poly-Si, such as ribbons, sheets and cast ingots [1 - 3]. Parallel to the work on these new crystallization methods, which are generally based on the use of high purity (semiconductor grade) silicon, runs the development of solar grade silicon [4, 5]. Although at present there is no clear definition of this term, it could be described as "optimized for use in solar cells" (instead of for use in integrated circuits), which refers mainly to purity in relation to price. Whereas (cast) poly-Si has been available for several years now, there is as yet no commercially produced solar grade silicon.

When poly-Si and solar grade silicon are introduced in solar cell manufacturing, it is necessary to optimize the processes used. In the case of poly-Si this is already being done, mainly for standard cell processes. As far as junction formation is concerned, these processes have in common the requirement of relatively high temperatures (typically 900 °C). It is known that high temperature processing adversely influences material quality, especially the

0379-6787/87/$3.50

minority carrier diffusion length [1, 6 - 8]. A decrease in the diffusion length results in a decrease in solar cell performance. This effect becomes more important when polycrystalline and less purified materials are used instead of high purity single-crystal silicon, because grain boundaries may be activated [9 - 11] and other defects may be created or activated [7, 12 - 14] during heating and cooling.

In order to avoid high temperatures, several techniques are being developed for cold junction processing, which means that junctions may be formed without appreciable heating of the bulk (base) material. This can be achieved by employing ion implantation and pulsed energy beams (lasers or electron beams) [15 - 21] which heat the surface very fast (typically in less than 1 μs), so that emitter dopants can be activated or driven in without the underlying material being affected.

In order to demonstrate the importance of this method of cold junction processing, in the present paper we compare cells which have been processed using high temperatures and cells which have been processed at low temperatures. The material used was semiconductor grade poly-Si. Phosphorus implantation was employed followed by either thermal annealing (TA) at a maximum temperature of 900 °C, or low temperature processing using pulsed excimer laser annealing (PLA) [16, 17].

2. Experimental details

The material used in this experiment was 5 cm × 5 cm cast polycrystalline Wacker–SILSO, doped p-type to a concentration of about 10^{16} cm^{-3}. No mechanical polishing was applied to this material. All wafers were selected from one part of an ingot and were neighbours. In this way the natural spread in cell parameters due to differences in grain structure and diffusion length was minimized and a comparison between the two processes for junction formation in the same material is possible.

The first step in cell preparation is the removal of surface damage due to wafer sawing by means of a wet chemical etch. Although NaOH is the most commonly used etchant for cast poly-Si, it is less suitable in this situation. NaOH etches highly anisotropically and thus gives rise to a pronounced surface texture. This texture complicates the use of directed beams [22], in this case the ion beam used for implantation and the excimer laser beam used for annealing of implantation damage. Therefore, to obtain a smooth surface finish, an HF:HNO_3:CH_3COOH (volume ratio, 1:5:2) mixture was used. The thickness of the as-sawn wafers was 400 μm; during etching 40 μm was removed from each side.

The front side of all the wafers was implanted at room temperature with phosphorus (ion energy, 10 keV; dose, 3×10^{15} cm^{-2}) while the back side was implanted with boron (ion energy, 20 keV; dose, 3×10^{15} cm^{-2}). During implantation, a 1 mm strip near the edges of the wafers was masked to avoid short-circuiting of the cells.

After implantation the wafers were divided into two sets. The front and back sides of the wafers of the first set (PLA) were annealed using an excimer laser. The annealing conditions for both sides were as follows: wavelength, 308 nm (XeCl); pulse length, about 20 ns (full width at half-maximum); energy density, 1.2 J cm^{-2}. During annealing, the wafers were kept at room temperature. The laser beam had a cross-section of 10 mm × 25 mm. For the irradiations, only the centre portion (4 mm × 18 mm) of the beam was used. This part of the beam showed a flat energy density profile and contained about 120 mJ. To anneal the entire 25 cm^2 area at the front and at the back of the wafers with the required energy density, the laser beam was focused and scanned over the wafers using a two-axis mirror scanner positioned at a distance of 50 cm from the wafers. The pulse energy available on the wafer (after focusing and reflection at three mirrors) was 100 mJ. A scan speed was chosen such that each spot overlapped the previous spot by at least 50%. Since the laser was operated at a repetition rate of 25 Hz, annealing of one side of a wafer could be performed within 2 min. The resulting sheet resistance of the emitter was about 30 Ω/□.

The wafers of the second set (TA) were thermally annealed in a vacuum furnace. The anneal consisted of two steps: 30 min at 600 °C, followed by 15 min at 900 °C. The heating rate was about 1 °C s^{-1}, and the cooling rate was about 0.25 °C s^{-1}. In this way an emitter sheet resistance of about 50 Ω/□ was obtained.

Electron beam evaporated Ti–Pd–Ag grids with a 10% coverage (optimized for a sheet resistivity of 30 Ω/□) were applied to all wafers. These contacts were sintered in vacuum at 400 °C for 10 min. No antireflective coating was applied.

Cell performance was measured at 25 °C under air mass (AM) 1 illumination. To evaluate the origin of differences in short-circuit current, additional measurements were done after passing the AM 1 light through a red filter (transparent to wavelengths greater than 600 μm) and a blue filter (transparent to wavelengths less than 600 μm). Thus the characteristics of the top and base regions of the cells could be distinguished. Additional information about the cell behaviour was obtained by applying a curve-fitting procedure [23] to the measured current–voltage (I–V) characteristics. In this way series and shunt resistances and diode saturation currents could be determined.

3. Results and discussion

We have processed four cells in each of the two sets. The I–V characteristics of two typical cells (area 25 cm^2) prepared on two neighbouring wafers using the two different methods of junction preparation as described above are shown in Fig. 1. The full lines drawn through the measured curves represent results of computer fits according to the double-exponential model [24, 25] shown schematically in Fig. 2. The most important measured and calculated parameters corresponding to the I–V measurements and simulations are given in Table 1. For the two batches of cells average results are shown. The standard deviations (in parentheses) show that the results were reproducible. In addition, this table gives the average I_r and I_{bl}, the short-circuit currents measured after passing AM 1 light through a red and a blue filter respectively.

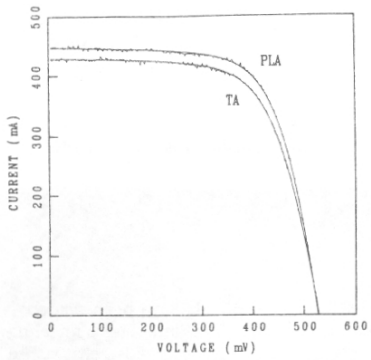

Fig. 1. Typical current–voltage characteristics of cells processed by ion implantation and subsequent laser annealing (PLA) or by thermal annealing (TA) in vacuum. The curves were measured under AM 1 illumination of 1000 W m^{-2}. The results from curve-fitting according to the model of Fig. 2 are shown as full lines drawn through the experimental curves.

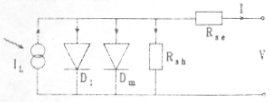

Fig. 2. Two-diode representation of a p–n junction solar cell under illumination: I_l, light-generated current; D_1, diode with quality factor 1; D_m, diode with quality factor $m > 1$; R_{sh}, shunt resistance; R_{se}, series resistance; I, current through cell terminals; V, voltage over cell terminals.

$$I = I_l - I_{01}(\exp \gamma V' - 1) - I_{0m}\left(\exp \frac{\gamma V'}{m} - 1\right) - \frac{V'}{R_{sh}}$$

$$\gamma = \frac{e}{kT} \qquad V' = V + IR_{se}$$

In Fig. 1 and Table 1 it is seen that the open-circuit voltage obtained on cells of the first set (PLA) is almost equal to that obtained on cells of the second set (TA), indicating that the behaviour of the junction made by ion implantation and pulsed excimer laser annealing is very similar to the behaviour of the junction made by ion implantation and thermal annealing. This is

TABLE 1

Averaged measured cell parameters and results from curve-fitting to a double-exponential model. The standard deviations are given in parentheses

Cell parameter	*Symbol*	*Pulsed laser-annealed (PLA) cells*	*Thermally annealed (TA) cells*
Open-circuit voltage	V_{oc} (mV)	530(1)	530(1)
Short-circuit current	I_{sc} (mA)	453(2)	437(3)
Short-circuit current (AM 1 filtered for $\lambda > 600$ nm)	I_r (mA)	250(1)	234(3)
Short-circuit current (AM 1 filtered for $\lambda < 600$ nm)	I_{bl} (mA)	115(1)	113(1)
Fill factor	FF (%)	68(1)	65(1)
Series resistance	R_{se} (mohm)	92(3)	117(1)
Shunt resistance	R_{sh} (ohm)	48(6)	30(10)
Diode saturation current (Quality factor 1)	I_{01} (nA)	0.25(0.02)	0.24(0.01)
Diode saturation current (Quality factor m)	I_{0m} (μA)	7.1(0.1)	6.9(0.1)
Quality factor	m	2	2
Light-generated current	I_l (mA)	453(2)	441(5)

also illustrated by the results of curve-fitting, which show that the curves for both types of cells can be fitted well using the same value for the quality factor m and approximately the same diode saturation currents. The average short-circuit currents, however, differ by about 16 mA. The current of the laser-annealed cell is higher than that of the thermally annealed cell. This difference is mainly caused by a difference in the current I_r generated by the long wavelength part of the spectrum, which is absorbed in the base region of the cell and which is higher for laser-annealed cells than for thermally annealed cells (see Table 1). No significant differences are observed in the current I_{bl} generated in the top layer of the cell. Therefore the lower short-circuit current of thermally annealed cells reflects base-region properties rather than emitter properties. As far as the base region is concerned, the only difference between laser annealing and thermal annealing is the temperature during processing. In the first case, for the bulk of the material, the temperature is close to room temperature during the entire process, whereas in the second case this temperature is high (maximum 900 °C) during processing. Apparently the minority carrier diffusion length in the base region is reduced on annealing at 900 °C.

The minority carrier diffusion length is strongly influenced by recombination processes at grain boundaries and intra-grain defects. Here carbon or

oxygen impurities from the crucible in which the material is cast, intrinsic (metallic) impurities or structural defects might play a role. As the nature of these defects and impurities is very complex, it is not possible to attribute the decrease in diffusion length to specific processes. Whatever the exact mechanisms might be, it is evident that for this material the high temperature processing employed here results in the formation or activation of recombination centres.

The slope of the I–V curve near $V = V_{oc}$ is less steep for curve TA than for curve PLA because of a higher value for the series resistance, as is seen in Table 1, and reflects the higher emitter sheet resistivity obtained after thermal annealing. As the sheet resistivity is determined by the majority carrier concentration and the carrier mobility, it is concluded that the active fraction of carriers or the carrier mobility is higher for a laser-annealed emitter than for a thermally annealed emitter. The average difference in fill factor between laser-annealed cells and thermally annealed cells is 3%, and is due to the differences in series resistance (2%) and shunt resistance (1%).

4. Conclusions

Wacker–SILSO poly-Si solar cells made by phosphorus implantation and pulsed excimer laser annealing yield a short-circuit current which is typically 3% - 4% higher than that for comparable cells made by phosphorus implantation and thermal annealing in vacuum at a maximum temperature of 900 °C. This difference originates from a decrease in the current generated in the base region of the cell upon thermal annealing. The electrical behaviour of junctions produced by both techniques is almost identical, as is illustrated by the results from curve fitting to a double-exponential model. Therefore equal open-circuit voltages are obtained with both techniques. Using the same implanted dose, the emitter sheet resistivity obtained by laser annealing is considerably lower than that obtained by thermal annealing.

Although in this work the material used was semiconductor grade, low temperature junction processing for polycrystalline silicon yields cells with a higher current output than high temperature processing. This can be partly related to intrinsic impurities. In that case the temperature effect is expected to become more pronounced when, in future, solar grade material will be used.

Acknowledgments

The authors wish to thank Ronald van Zolingen and Bert Habraken for their valuable contribution to this work and for many discussions. Simon Doorn is acknowledged for the ion implantations, Gerrit Frijlink for the evaporation of contacts.

This work is part of the research program of the Stichting voor Fundamenteel Onderzoek der Materie and was financially supported by the Nederlandse Organisatie voor Zuiver Wetenschappelijk Onderzoek.

References

1 E. Fabre, in W. H. Bloss and G. Grassi (eds.), *Proc. 4th Commission of the European Communities Conf. on Photovoltaic Solar Energy, 1982*, Reidel, Dordrecht, 1982, p. 346.
2 J. G. Grabmaier, in W. Palz and F. C. Treble (eds.), *Proc. 6th Commission of the European Communities Conf. on Photovoltaic Solar Energy, 1985*, Reidel, Dordrecht, 1985, p. 922.
3 C. F. A. van Os, J. L. P. W. Verpalen and J. Bezemer, *Sol. Energy Mater., 10* (1984) 209.
4 J. Grabmaier (ed.), *Crystals (5): Silicon*, Springer, Berlin, 1981.
5 H. A. Aulich, in W. Palz and F. Fittipaldi (eds.), *Proc. 5th Commission of the European Communities Conf. on Photovoltaic Solar Energy, 1983*, Reidel, Dordrecht, 1984, p. 936.
6 B. O. Seraphin (ed.), *Solar Energy Conversion: Solid State Physics Aspects*, Springer, Berlin, 1979, p. 173.
7 C. T. Ho and F. V. Wald, *Phys. Status Solidi A, 67* (1981) 103.
8 M. B. Spitzer, C. J. Keavney, R. G. Wolfson and R. J. Matson, *Proc. 17th IEEE Conf. Photovotaic Specialists, Kissimmee, FL, 1984*, IEEE, New York, 1984, p. 252.
9 D. Redfield, *Appl. Phys. Lett., 38* (1981) 174.
10 L. L. Kazmerski, in W. Palz and F. Fittipaldi (eds.), *Proc. 5th Commission of the European Communities Conf. on Photovoltaic Solar Energy, 1983*, Reidel, Dordrecht, 1984, p. 40.
11 G. B. Turner, D. Tarrant, D. Aldrich, R. Pressley and R. Press, *Proc. 16th IEEE Conf. Photovoltaic Specialists, San Diego, CA, 1982*, IEEE, New York, 1982, p. 775.
12 J. G. Fossum and D. S. Lee, *Proc. 15th IEEE Conf. Photovoltaic Specialists, Kissimmee, FL, 1981*, IEEE, New York, 1981, p. 120.
13 C. Claeys, H. Bender, G. Declerck, J. van Landuyt, R. van Overstraeten and S. Amelinckx, in C. A. J. Ammerlaan (ed.), *Proc. 12th Int. Conf. on Defects in Semiconductors*, North-Holland, Amsterdam, 1983, p. 148.
14 K. V. Ravi, *Imperfections and Impurities in Semiconductor Silicon*, Wiley-Interscience, New York, 1981.
15 J. M. Poate and J. W. Mayer (eds.), *Laser Annealing of Semiconductors*, Academic Press, New York, 1982.
16 J. M. Poate and W. L. Brown, *Physics Today*, June (1982) 24.
17 R. T. Young, Energy beam–solid interactions and transient thermal processing, in J. C. C. Fan and N. M. Johnson (eds.), *Materials Research Society Symposia Proceedings*, Vol. 23, North-Holland, New York, 1984, p. 217.
18 A. C. Greenwald, A. R. Kirkpatrick, R. G. Little and J. A. Minucci, *J. Appl. Phys., 50* (1979) 783.
19 R. T. Young and R. F. Wood, *Proc. 14th IEEE Conf. Photovoltaic Specialists, San Diego, CA, 1980*, IEEE, New York, 1980, p. 214.
20 M. Finetti, P. Ostoja, S. Solmi and Q. Zini, *Sol. Cells, 2* (1980) 101.
21 C. T. Ho, G. Moeller, F. V. Wald and M. B. Spitzer, *Sol. Cells, 11* (1984) 29.
22 W. Sinke, W. van Sark, S. Doorn, F. W. Saris, J. Donon, P. Loubly and G. David, in W. Palz and F. Fittipaldi (eds.), *Proc. 5th Commission of the European Communities Conf. on Photovoltaic Solar Energy*, Reidel, Dordrecht, 1984, p. 1095.
23 A. Polman, W. G. J. H. M. van Sark, W. Sinke and F. W. Saris, *Sol. Cells, 17* (1986) 241.
24 S. C. Choo, *Solid-State Electron., 11* (1968) 1069.
25 M. Wolf, G. T. Noel and R. J. Stirn, *IEEE Trans. Electron Devices, 24* (1977) 419.